Anthropogenic signatures of lead in the Northeast Atlantic

Authors: D. Rusiecka[1,2], M. Gledhill[1,2], A. Milne[3], E.P. Achterberg[1,2], A.L. Annett[4], S. Atkinson[3], A. Birchill[3], J. Karstensen[2], M. Lohan[3,1], C. Mariez[5], R. Middag[6], J. M. Rolison[7], T. Tanhua[2], S. Ussher[3], and D. Connelly[8]

[1]Ocean and Earth Sciences, National Oceanography Centre, University of Southampton, Southampton, UK, [2]GEOMAR Helmholtz Centre for Ocean Research Kiel, Germany, [3]School of Geography, Earth and Environmental Sciences, University of Plymouth, Plymouth, UK, [4]School of GeoSciences, University of Edinburgh, Edinburgh, UK, [5]Université de Bretagne Occidentale, France, [6]NIOZ Royal Netherlands Institute for Sea Research, Department of Ocean Systems, Netherlands, [7]Nuclear and Chemical Sciences Division, Lawrence Livermore National Laboratory, Livermore, USA, [8]National Oceanography Centre Southampton, European Way, Southampton, UK

Corresponding authors: Dagmara Rusiecka (drusiecka@gmail.com) and Eric Achterberg (eachterberg@geomar.de)

Key Points:

- Recent sources of Pb were evident despite a 4–fold reduction of Pb in NE Atlantic surface waters since leaded gasoline prohibition
- Enhanced Pb was evident in Mediterranean Outflow Waters, transported >2500 km across the NE Atlantic
- Sediments represented an important source of Pb to overlying waters, exceeding the atmospheric flux of Pb

This article has been accepted for publication and undergone full peer review but has not been through the copyediting, typesetting, pagination and proofreading process which may lead to differences between this version and the Version of Record. Please cite this article as doi: 10.1002/2017GL076825

Abstract

Anthropogenic activities have resulted in enhanced lead (Pb) emissions to the environment over the past century, mainly through the combustion of leaded gasoline. Here, we present the first combined dissolved (DPb), labile (LpPb) and particulate (PPb) Pb dataset from the Northeast Atlantic (Celtic Sea) since the phasing out of leaded gasoline in Europe. Concentrations of DPb in surface waters have decreased by 4-fold over the last four decades. We demonstrate that anthropogenic Pb is transported from the Mediterranean Sea over long distances (>2500 km). Benthic DPb fluxes exceeded the atmospheric Pb flux in the region, indicating the importance of sediments as a contemporary Pb source. A strong positive correlation between DPb, PPb and LpPb indicates a dynamic equilibrium between the phases and the potential for particles to 'buffer' the DPb pool. This study provides insights into Pb biogeochemical cycling and demonstrates the potential of Pb in constraining ocean circulation patterns.

1 Introduction

Lead (Pb) is one of few elements for which the impact of human activity on the marine environment is clearly evident. Anthropogenic perturbation of the natural biogeochemical cycle of Pb in the ocean dates back to ~1850 (Kelly et al. 2009), with coal and leaded gasoline combustion serving as major sources of Pb to the atmosphere (Kelly et al. 2009; Wu & Boyle 1997). Anthropogenic Pb is transported in the atmosphere in the form of fine aerosol particles that can travel long distances, and are deposited in remote areas resulting in enhanced DPb surface ocean concentrations (Kumar et al. 2014; Véron & Church 1997), reaching >190 pmol kg^{-1} during the peak of the Pb emissions in 1970-80 (Laumond et al. 1984). Anthropogenic Pb has entirely masked signals of naturally sourced Pb (ca. 2.2 pmol kg^{-1} in surface waters (Henderson & Maier-Reimer 2002)). To date, leaded gasoline has been virtually phased out (except in 3 countries, as of March 2017, UNEP), and Pb concentrations have decreased significantly from ~170 to <15 pmol kg^{-1} in surface waters (Boyle et al. 2014; Schaule & Patterson 1983), leading to recent evidence for natural Pb signatures re-emerging in the North Atlantic (Bridgestock et al. 2016).

The spatial and temporal variable historic Pb inputs to the marine environment can be used to investigate the reactivity and cycling of this element, and trace long-range ocean circulation patterns (Chen et al. 2016; Fine 2010; Lee et al. 2015). Anthropogenic Pb has been utilised as a tracer of subducted surface waters in the Indian (Lee et al. 2015) and Pacific Oceans (Chien et al. 2017), and ventilated surface waters of the Northwest Atlantic (Boyle et al. 2014). Anthropogenic perturbation of natural Pb concentrations in the ocean has been described as an '*evolving global experiment'* (Boyle et al. 2014) that demonstrates the magnitude of human impact on the environment.

Lead is a particle reactive element in marine waters and is typically removed through scavenging, with the sediments acting as repositories. However, the role of particulate matter and the physico-chemical processes that influence the fate of dissolved Pb (DPb) and facilitate long-range transport are poorly constrained. A slow release of DPb from particles and a rapid isotopic exchange with particulate matter that can influence the fate of particulate Pb (PPb) has recently been reported (Chen, Boyle, et al. 2016). Therefore, in order to gain insights into biogeochemical cycling of Pb in the marine environment, both phases should be considered.

Here we report and evaluate the first extensive seasonal study of DPb, PPb and leachable Pb (LpPb) distributions in Northeast Atlantic marginal seas since the phase-out in Europe of leaded gasoline use in 1980 – 2011 (European Communities 1978; Economic Commission for Europe 2014). This study provides insights into the dynamic relationship between

dissolved and particulate phases and demonstrates the role of benthic Pb release and Pb as a tracer of North Atlantic circulation patterns.

2 Study region, materials and methods

Full details of the study region, sampling and methods are provided in the supporting information (SI) (S1). Briefly, samples for trace metal analysis were collected during three different seasons; November – December 2014 (DY018), April 2015 (DY029), and July – August 2015 (DY033) in the Northeast Atlantic continental margin (Celtic Sea) (Fig. 1), on board *RRS Discovery*. Two off-shelf transects were conducted along a canyon (T1_C, stations C01 – C07, C15), nearby a spur (T2_S, stations S08 – S09) (SI, S1) and one on-shelf transect in the Celtic Sea (stations CS2, CCS, J02 – J06, Site A). Trace metal samples were collected following GEOTRACES protocols (Cutter et al. 2010). Dissolved Pb and Mn (DMn) were filtered using a 0.2 μm cartridge filter (Sartobran 300, Sartorius), preconcentrated using an automated system (SC-4 DX SeaFAST pico; ESI) and analysed by high-resolution inductively coupled plasma-mass spectrometry (HR-ICP-MS; Thermo Fisher Element XR) (Rapp et al. 2017). Dissolved Fe (DFe) (0.2 μm filtered) was analyzed by flow injection with chemiluminescence detection (Obata et al. 1993) as detailed in (Birchill et al. 2017). Particulate Pb was collected on clean 25 mm Supor® polyethersulfone membrane disc filters (Pall, 0.45 μm) and subjected to a 25% acetic acid-hydroxylamine hydrochloride leach (LpPb) (Berger et al. 2008) and subsequently an acid digestion (PPb) (Ohnemus et al. 2014). Particulate samples were analysed using ICP-MS (Thermo Fisher X Series 2). Dissolved aluminium (DAl) (0.2 μm filtered) was analyzed using spectrofluorometry following the method by Hydes and Liss (1976). Evaluation of the accuracy and efficiency of these methods was carried out using Certified Reference Materials with the results showing good agreement (SI, Table 1). Some data points were identified as outliers and were excluded from consideration (SI, S2). Radium (Ra) isotopes ^{223}Ra and ^{224}Ra were extracted from large seawater volumes (60 – 100 L) by adsorption onto Mn acrylic fibers (Sun & Torgersen 1998). Ra activities were analyzed at sea by Radium Delayed Coincidence Counting following standard methodology (Annett et al. 2013; Garcia-Solsona et al. 2008; Moore 2008; Moore & Arnold 1996). Ra activities used here ($^{224}Ra_{xs}$ and $^{223}Ra_{xs}$) are in excess of activity supported by the parent isotopes in the water column (SI, S1). Water mass distribution was quantified using extended Optimum Multiparameter analysis (extOMP) (Hupe & Karstensen 2000; Karstensen & Tomczak 1998; Pollard et al. 2004). The propagation time of MOW from the Gulf of Cadiz was calculated analogously to (Waugh et al. 2003), using CFC-12 data available in the GLODAPv2 data product (Olsen et al. 2016). Aerosol samples were digested using HF and HNO_3 following the method adapted from (Morton et al. 2013), and analysed by the ICP-MS (Thermo Fisher X Series 2). Section plots figures were created with Ocean Data View (2015) software (Schlitzer 2015) with DIVA gridding settings.

3 Results and discussion

DPb concentrations in the Celtic Sea region ranged between 29.6 and 122 pmol kg^{-1} (Fig. 2a-c and Fig. S1). Off-shelf distributions showed elevated DPb concentrations (50.8 ± 3.0 pmol kg^{-1} (n = 20)) in the seasonal mixed layer (SML) along the canyon transect in November, and also at stations S08 and S09 along the spur transect. Below the SML, DPb distributions were generally consistent along both transects for all seasons and decreased down to 38 pmol kg^{-1} in the subsurface waters and increased at depths of ~ 550 – 1500 m to 46.6 ± 5.6 pmol kg^{-1} (n = 84). In deeper waters (> 1500 m), DPb concentrations decreased to 37.0 ± 3.2 pmol kg^{-1} (n = 39). On the continental shelf, DPb concentrations were generally

higher in comparison to the off-shelf transects and ranged between 36.1 – 122 pmol kg^{-1}. Elevated DPb concentrations were measured in surface waters in April (96.8 pmol kg^{-1}) and July (99.1 pmol kg^{-1}) with somewhat lower levels in November (72.6 pmol kg^{-1}), whereas DPb was persistently elevated in bottom waters (up to 121 pmol kg^{-1}) across all seasons. No correlations between DPb and macronutrients were observed.

Our surface water DPb concentration of 40.2 ± 7.5 pmol kg^{-1} (n = 109) along the shelf break in 2014-2015 showed at least a 4-fold decrease compared to previous reports for the region (. 2 e, Table S2) (Brügmann et al. 1985; Cotté-Krief et al. 2002; Helmers & Van der Loeff 1993; Lambert et al. 1991; Muller et al. 1994), and were generally lower in comparison to other European shelf waters over the last 4 decades (Kremling & Streu 2001; Laumond et al. 1984; Monteiro et al. 2015; Pohl et al. 2011; Prego et al. 2013; Waeles et al. 2008). The diminishing DPb concentrations over the last 2 decades form a success of the phase-out process of leaded gasoline. Nevertheless, the observed concentrations in our study region exceeded predicted natural levels of Pb (Henderson & Maier-Reimer 2002) by at least an order of magnitude, indicating that the vast majority of Pb still has an anthropogenic origin. Thus, the elevated DPb concentrations we report in surface waters indicate the presence of recent anthropogenic Pb inputs to Northeast Atlantic waters from sources such as coal burning, smelting or mining (Nriagu & Pacyna 1988; Lee et al. 2014).

3.1 Long range Pb transport in MOW

Elevated DPb concentrations of 46.6 ± 5.6 pmol kg^{-1} (n = 84) were a persistent feature in the depth range ~550 – 1500 m (27.30 – 27.75 kg m^{-3} σ_0) in the slope region of the Celtic Sea. The DPb maximum coincided with salinity (35.74) (Fig. 3a) and DAl (17.3 ± 2.6 nmol kg^{-1}, n = 88) maxima (Fig. S2), signatures of Mediterranean Outflow Water (MOW) (Measures & Edmond 1988; Rolison et al. 2015). Surface waters in the Mediterranean Sea received enhanced atmospheric Pb inputs during the period of leaded gasoline use, with maximum surface DPb of >190 pmol kg^{-1} (Laumond et al. 1984). Mediterranean waters also receive enhanced aeolian fluxes of Al from Saharan dust (Rolison et al. 2015). Deep water formation occurs in the Levantine Basin and Gulf of Lions, and the saline deep Mediterranean waters with enhanced DPb (40 - 80 pmol kg^{-1}) (Rolison 2016) and DAl (125 – 170 nmol kg^{-1} (Rolison et al. 2015)) exit the Strait of Gibraltar as bottom waters and mix with ENACW (García-Ibáñez et al. 2015). The MOW spreads across NE Atlantic at a depth ~550 – 1500 m and propagates along the continental slope towards the Celtic Sea shelf break. The mean propagation time of MOW from the Gulf of Cadiz to the Celtic Sea slope region is ~5 years (Fig. S3). The presence of MOW at intermediate depths in the study region has previously been reported (Cotté-Krief et al. 2002; Lambert et al. 1991) and was confirmed by the extOMP analysis (Fig. 3b and Fig. S4). The core of the MOW (up to 55%) was identified at ~1000 m depth with a Gaussian decay (20% at 550 m and 1500 m).

Enhanced DPb concentrations were also observed along GEOTRACES transects in corresponding MOW density layers (27.22 – 27.82 kg m^{-3} σ_0): in the Gulf of Cadiz (49.0 ± 2.6 pmol kg^{-1}, n = 14, GA04 (Rolison 2016)), north (46.1 ± 6.1 pmol kg^{-1}, n = 18, GA01) and south of the Gulf of Cadiz (55.1 ± 5.5 pmol kg^{-1}, n=10, GA03, (Noble et al. 2015)) (Fig. S5), in agreement with our observations. Our study region is ~2500 km away from the Strait of Gibraltar, therefore the concentration of DPb and DAl may be expected to decrease through scavenging and/or dilution processes during transit. Whilst DAl concentrations and salinity correlated well (r^2 = 0.68) and decreased from 27.8 ± 7.2 nmol kg^{-1} and 35.6-36.4 (Gulf of Cadiz) to 17.3 ± 2.6 nmol kg^{-1} and 35.4-35.7, there was no correlation of DPb with salinity and DPb concentrations remained unchanged (Fig. S6). We suggest the following processes

that maintain elevated DPb signal during MOW transit: i) benthic inputs from the European continental slopes. Shelf break sediments have been suggested as a Pb source in the Philippine Sea (Chien et al. 2017). Local sediment resuspension events in the Bay of Biscay as MOW propagates along the continental slope have also been reported (McCave & Hall 2002). ii) Reversible Pb sorption onto particle surfaces. This mechanism has been suggested to supply DPb to North Pacific deep waters (Wu et al. 2010). Pb isotope exchange between these two phases has been demonstrated (Chen et al. 2016; Sherrell et al. 1992) and the potential of particle reversible sorption has been shown using thorium isotopes (Bacon & Anderson 1982). Potentially, DPb (< 0.2 μm) may be released from particles in the form of small, low specific density inorganic particles (colloids 0.02 – 0.2 μm) with longer residence time. However, PPb dissolution within MOW is also plausible. Our results show that the major portion of PPb was in LpPb form (78 ± 10%, n = 205) while overall the majority of the total Pb pool (PPb + DPb) was in the DPb fraction (70 ± 18%, n = 171), thus implying a significant role of particles in DPb distributions.

Partial mixing with other historically Pb polluted waters, such as Northeast Atlantic ventilated surface waters and LSW transported across the North Atlantic (Bridgestock et al. 2018; Zurbrick et al. 2018), has been shown to influence DPb concentrations at intermediate depths and thus also need to be considered. Low-salinity, and high-oxygen LSW underlies the warm, saline MOW (Talley & McCartney 1982). Our extOMP confirmed a layering of the water masses with MOW at a core depth 27.60 kg m^{-3} transiting into the LSW core at 27.79 kg m^{-3} (Fig S4) and a potential for vertical mixing of bottom layers of MOW with LSW. Within waters identified as LSW (27.76 – 27.85 kg m^{-3} σ_0), concentrations of DPb (42.9 ± 4.5 pmol kg^{-1} (n = 42)) and DAl (15.8 ± 1.0 nmol kg^{-1} (n = 40)) were somewhat lower, and salinity (34.98 – 35.4) and temperature (from 8.8 ± 1.5 to 5.1 ± 1.0 ^{o} C) were lower in comparison to overlying MOW. These values were higher in comparison to DPb (36.9 ± 7.4 pmol kg^{-1}, n = 60), DAl (13.0 ± 1.2 nmol kg^{-1}, n = 60), salinity (34.94 – 35.2) and temperature (4.3 ± 0.6 ^{o}C) observed within LSW (27.68 – 27.81 kg m^{-3} σ_0) in the NW Atlantic (GA02 section, 2010) (Mawji et al. 2015). Densities of MOW and LSW are similar and a complete differentiation is therefore challenging, preventing us from determining the exact fraction of each water mass. Our findings indicate the potential for MOW penetration into deeper waters, altering properties of LSW although the upward vertical mixing cannot be ruled out. We conclude that the DPb maximum in the Celtic Sea region was a result of anthropogenically perturbed MOW masses reaching NE Atlantic continental margins.

3.2 Sediment release of a particle reactive element

Elevated DPb (65.9 – 121 pmol kg^{-1}) and PPb concentrations (149 – 806 pmol kg^{-1}) were observed in bottom waters at Site A during all seasons, and on the continental slope at C03-C04 stations in November (DPb: 52.5 ± 5.6 pmol kg^{-1}, n = 7, PPb: 29.3 ± 13.9 pmol kg^{-1}, n = 8) (Fig. 4). Following fluvial or atmospheric inputs to marine waters, Pb is typically scavenged and transferred to the seafloor (Bastami et al. 2015; Marani et al. 1995). Tidal currents, wind driven waves and storm events cause resuspension of sediments (Kalnejais et al. 2007), thereby supplying Pb-enriched porewaters and particles to the water column. This mechanism has been reported for deep ocean (Lee et al. 2015; Noble et al. 2015), coastal (Annibaldi et al. 2009; Chien et al. 2017), estuarine (Rivera-Duarte & Flegal 1994), and riverine systems (Ferrari & Ferrario 1989), and observed in sediment chamber experiments (Kalnejais et al. 2007; Zago et al. 2000).

At Site A, the enhanced DPb and PPb concentrations near the seafloor coincided with persistently elevated turbidity signals (Fig. 4), indicating particle resuspension and subsequent DPb and PPb remobilization from the sediments to overlying waters. The benthic

Pb supply is supported by increased levels of the short-lived isotopes $^{223}Ra_{xs}$ and $^{224}Ra_{xs}$ (half-lives 3.66 and 11.4 days, respectively) near the seafloor (Fig. 4), indicating recent sedimentary supply. A similar feature was observed on the continental slope along the canyon transect in November where salinity maximum associated with MOW decreased towards the continental shelf break (Fig. 3a) from 35.74 (C01) to 35.61 (C04) (~1000 m depth) thus DPb concentrations were also expected to decrease. Yet DPb concentrations remained unchanged (Fig. 2a) and PPb concentrations were elevated, coinciding with increased $^{223}Ra_{xs}$, $^{224}Ra_{xs}$ and turbidity signals (Fig. 4 and Fig. S7), indicating a sedimentary Pb source to overlying waters.

Benthic DPb remobilization has been reported by (Noble et al. 2015) and (Chien et al. 2017). To our knowledge, we provide the first clear evidence of a benthic Pb source supported by PPb and Ra field measurements. Furthermore, our results showed a strong positive correlation between DPb and PPb ($r^2 = 0.97$, n = 12), and DPb and LpPb ($r^2 = 0.97$, n = 12) at Site A and C03/C04 stations (Fig. S8), indicating a dynamic equilibrium between the phases. Although, little is known about biogeochemical processes facilitating DPb sedimentary release, we suggest that benthic remobilization could be facilitated through Pb association with Fe/Mn oxi-hydroxide precipitates (Allen et al. 1990; Bastami et al. 2015; Fernex et al. 1992; Kalnejais et al. 2007) with subsequent reductive dissolution of the solid Fe and Mn forms in sediments (Fernex et al. 1992). This mechanism is supported by elevated DFe and DMn concentration towards the seafloor (Fig. S9) and a build up of Fe(II) in sediments at Site A (Klar et al. 2017), but not at stations C03/C04. Potentially, DPb may be supplied in the form of small colloids deposited onto sediments (Muller 1996; Sen & Khilar 2006), with these Pb-enriched resuspended fine particles having a longer residence time in comparison to bulk sediment particles (Ferrari & Ferrario 1989; Kalnejais et al. 2007).

We determined a benthic Pb flux to overlying waters of 27 - 41 x 10^{-9} moles Pb m^{-2} d^{-1} (n = 3) at Site A in April (SI, S4) using short-lived Ra isotopes (Moore 2000). To our knowledge, this is the first benthic Pb flux estimate from field observations. Furthermore, this sedimentary Pb flux was up to 2 orders of magnitude higher than the atmospheric flux (0.03 – 12.2 x 10^{-9} moles Pb m^{-2} d^{-1}) observed at nearby Penlee Point Atmospheric Observatory in 2015 (Fig. 1 and S5 (Arimoto et al. 2003)). The benthic DPb flux was likely a result of accumulation in sediments of Pb deposited over time, whilst the recent relatively low atmospheric Pb flux reflects the implementation of strict European air emission regulations. We therefore stress that sediments containing legacy Pb will continue to serve as an important, if not the major source of Pb to overlying waters.

3.3 Recent Pb sources in the NE Atlantic shelf region

A strong spatial and temporal variability in surface water DPb concentrations were observed over the various transects across the seasons. Elevated surface DPb concentrations (36.1 – 122 pmol kg^{-1}) were observed on the continental shelf during all sampling seasons, with lower levels along off-shelf transects (Fig. 2c). Elevated DPb concentrations observed in surface waters at Site A in April and July in comparison to November, indicated recent Pb inputs (Fig. 4). A strong inverse correlation of DPb with salinity r = -0.96 (April, n = 6) and r = -0.94 (July, n = 4) between Site A and CS2 stations suggest a freshwater source of DPb, which could be continental run-off or wet deposition (Fig. S10). On the continental slope, elevated DPb concentrations in the SML were observed along the canyon (T1_C) transect in November (50.8 ± 3.0 pmol kg^{-1}, n = 20) and at S08 and S09 stations on the spur (T2_S) transect. Lower DPb concentrations were observed during other seasons; 39.6 ± 6.9 pmol kg^{-1} (n = 23, T1_C) and 35.0 ± 4.2 pmol kg^{-1} (n = 30, T2_S) in April and 35.2 ± 3.8 pmol kg^{-1} (n

= 9, T1_C) and 37.4 ± 4.9 pmol kg^{-1} (n = 6, T2_S) in July (Fig. 2a-b). The distinctive changes in DPb over short spatial scale observed between our closely spaced stations (<20 km), suggest presence of different water masses with different DPb input histories over the last months to years. These observations coincided with distinct temperature and DMn concentration differences (Fig. S11), that enforce this suggestion.

4 Conclusions

Our observations demonstrate the widespread impact of anthropogenic Pb emissions on the marine environment. The elevated Pb signal (46.6 ± 5.6 pmol kg^{-1}) in MOW is transported long distances (> 2500 km) at intermediate depths across the Northeast Atlantic following anthropogenic Pb emissions during the past century. Following implementation of stricter environmental regulations in Europe, this oceanic Pb signal will behave similarly to chlorofluorocarbons (CFCs) in that it is predicted to decrease with time. However, considering the residence time of Pb in the deep ocean of ~100 years (Nozaki & Tsunogai 1976), the presence of recent Pb sources (> 90 pmol kg^{-1} in surface waters) and the 're-supply' of Pb to the water column from sediments containing legacy Pb (27 - 41 x 10^{-9} moles Pb m^{-2} d^{-1}), we expect the anthropogenic Pb signal to remain in the marine environment for decades to come. The role of the particulate phase in buffering Pb concentrations in the water column needs to be considered in the interpretation of oceanic DPb distributions due to a close relationship between the dissolved and particulate phases.

Acknowledgments

This project was funded by the UK Natural Environment Research Council (NE/K001973/1 (E.A., M.G.), NE/K001779/1 (M.L.), NE/K002023/1 (A.A.), NE/L501840/1 (A.B.)). The authors declare no competing financial interests. The authors thank the captain and crew of *RRS Discovery* for their assistance during research expeditions, Malcolm Woodward and Carolyn Harrys for the macronutrient data. We thank Insa Rapp for the training in the sample analysis and Alex Zavarsky for the help with the Matlab scripts, Cheryl Zurbrick and Ed Boyle for the GA01 section dataset and their contribution to IDP 2017. The GA04 cruises were funded by the Netherlands Organization for Scientific Research (882.01.015). Analysis was funded by the University of Otago and the Royal Netherlands Institute for Sea Research. Data has ben submitted to BODC.

References

Allen, J. R. L., Rae, J. E., & Zanin, P. E. (1990). Metal Speciation (Cu, Zn, Pb) and Organic-Matter in an Oxic Salt- Marsh, Severn Estuary, Southwest Britain. *Marine Pollution Bulletin*, *21*(12), 574–580. https://doi.org/http://dx.doi.org/10.1016/0025-326X(90)90606-9

Annett, A. L., Henley, S. F., Van Beek, P., Souhaut, M., Ganeshram, R., Venables, H. J., et al. (2013). Use of radium isotopes to estimate mixing rates and trace sediment inputs to surface waters in northern Marguerite Bay, Antarctic Peninsula. *Antarctic Science*, *25*(3), 445–456. https://doi.org/10.1017/S0954102012000892

Annibaldi, A., Truzzi, C., Illuminati, S., & Scarponi, G. (2009). Recent sudden decrease of lead in Adriatic coastal seawater during the years 2000-2004 in parallel with the phasing out of leaded gasoline in Italy. *Marine Chemistry*, *113*(3–4), 238–249. https://doi.org/10.1016/j.marchem.2009.02.005

Arimoto, R., Duce, R. A., Ray, B. J., & Tomza, U. (2003). Dry deposition of trace elements to the western North Atlantic. *Global Biogeochemical Cycles*, *17*(1), n/a-n/a. https://doi.org/10.1029/2001GB001406

Bacon, M. P., & Anderson, R. F. (1982). Distribution of thorium isotopes between dissolved and particulate forms in the deep sea. *Journal of Geophysical Research: Oceans*, *87*(C3), 2045–2056. https://doi.org/10.1029/JC087iC03p02045

Bastami, K. D., Neyestani, M. R., Shemirani, F., Soltani, F., Haghparast, S., & Akbari, A. (2015). Heavy metal pollution assessment in relation to sediment properties in the coastal sediments of the southern Caspian Sea. *Marine Pollution Bulletin*, *92*(1–2), 237–243. https://doi.org/10.1016/j.marpolbul.2014.12.035

Berger, C. J. M., Lippiatt, S. M., Lawrence, M. G., & Bruland, K. W. (2008). Application of a chemical leach technique for estimating labile particulate aluminum, iron, and manganese in the Columbia River plume and coastal waters off Oregon and Washington. *Journal of Geophysical Research*, *113*, C00B01. https://doi.org/10.1029/2007JC004703

Birchill, A. J., Milne, A., Woodward, E. M. S., Harris, C., Annett, A., Rusiecka, D., et al. (2017). Seasonal iron depletion in temperate shelf seas. *Geophysical Research Letters*, *44*(17), 8987–8996. https://doi.org/10.1002/2017GL073881

Boyle, E., Lee, J., Echegoyen, Y., Noble, A., Moos, S., Carrasco, G., & Zhao, N. (2014). Anthropogenic Lead Emissions in the Ocean: The Evolving Global Experiment. *Oceanography*, *27*(1), 69–75.

Bridgestock, L., Rehkämper, M., van de Flierdt, T., Paul, M., Milne, A., Lohan, M. C., & Achterberg, E. P. (2018). The distribution of lead concentrations and isotope compositions in the eastern Tropical Atlantic Ocean. *Geochimica et Cosmochimica Acta*, *225*, 36–51. https://doi.org/https://doi.org/10.1016/j.gca.2018.01.018

Bridgestock, L., van de Flierdt, T., Rehkämper, M., Paul, M., Middag, R., Milne, A., et al. (2016). Return of naturally sourced Pb to Atlantic surface waters. *Nature Communications*, *7*, 12921. https://doi.org/10.1038/ncomms12921

Brügmann, L., Danielsson, L.-G., Magnusson, B., & Westerlund, S. (1985). Lead in the North Sea and the north east Atlantic Ocean. *Marine Chemistry*, *16*(1), 47–60. https://doi.org/10.1016/0304-4203(85)90027-1

Chen, M., Boyle, E. A., Lee, J., Nurhati, I., Zurbrick, C., Switzer, A. D., & Carrasco, G. (2016). Lead isotope exchange between dissolved and fluvial particulate matter: a laboratory study from the Johor River estuary. *Philosophical Transactions of the Royal Society A: Mathematical, Physical and Engineering Sciences*, *374*(2081), 20160054. https://doi.org/10.1098/rsta.2016.0054

Chen, M., Goodkin, N. F., Boyle, E. A., Switzer, A. D., & Bolton, A. (2016). Lead in the western South China Sea: Evidence of atmospheric deposition and upwelling. *Geophys.Res.Lett.*, 4490–4499. https://doi.org/10.1002/2016GL068697.Received

Chien, C. Te, Ho, T. Y., Sanborn, M. E., Yin, Q. Z., & Paytan, A. (2017). Lead concentrations and isotopic compositions in the Western Philippine Sea. *Marine Chemistry*, *189*, 10–16. https://doi.org/10.1016/j.marchem.2016.12.007

Cotté-Krief, M.-H., Thomas, A. J., & Martin, J.-M. (2002). Trace metal (Cd, Cu, Ni and Pb) cycling in the upper water column near the shelf edge of the European continental margin (Celtic Sea). *Marine Chemistry*, *79*(1), 1–26. https://doi.org/https://doi.org/10.1016/S0304-4203(02)00013-0

Cutter, G., Andersson, P., Codispoti, L., Croot, P., François, R., Lohan, M. C., et al. (2010). Sampling and Sample-handling Protocols for GEOTRACES Cruises, (December).

Economic Commission for Europe. (2014). *Convention on Long-range Transboundary Air Pollution*. Geneva, 52nd session, 30 June–3 July 2014.

European Communities. (1978). Council Directive 78/611/EEC of 29 June 1978 on the approximation of the laws of the Member States concerning the lead content of petrol. *Official Journal of the European Communities*, *L 197*, 19–21. https://doi.org/10.1039/ap9842100196

Fernex, F., Février, G., Bénaïm, J., & Arnoux, A. (1992). Copper, lead and zinc trapping in Mediterranean deep-sea sediments: probable coprecipitation with Mn and Fe. *Chemical Geology*, *98*(3–4), 293–306.

https://doi.org/10.1016/0009-2541(92)90190-G
Ferrari, G. M., & Ferrario, P. (1989). Behavior of Cd, Pb, and Cu in the marine deltaic area of the Po River (North Adriatic Sea). *Water, Air, and Soil Pollution*, *43*(3), 323–343. https://doi.org/10.1007/BF00279200
Fine, R. A. (2010). Observations of CFCs and SF6 as Ocean Tracers. *Annual Review of Marine Science*, *3*(1), 173–195. https://doi.org/10.1146/annurev.marine.010908.163933
García-Ibáñez, M. I., Pardo, P. C., Carracedo, L. I., Mercier, H., Lherminier, P., Ríos, A. F., & Pérez, F. F. (2015). Structure, transports and transformations of the water masses in the Atlantic Subpolar Gyre. *Progress in Oceanography*, *135*, 18–36. https://doi.org/10.1016/j.pocean.2015.03.009
Garcia-Solsona, E., Garcia-Orellana, J., Masqué, P., & Dulaiova, H. (2008). Uncertainties associated with 223Ra and 224Ra measurements in water via a Delayed Coincidence Counter (RaDeCC). *Marine Chemistry*, *109*(3–4), 198–219. https://doi.org/10.1016/j.marchem.2007.11.006
Helmers, E., & Van der Loeff, M. M. R. (1993). Lead and aluminum in Atlantic surface waters (50 degree N to 50 degree S) reflecting anthropogenic and natural sources in the eolian transport. *Journal of Geophysical Research*, *98*(C11), 20261–20273. https://doi.org/10.1029/93JC01623
Henderson, G. M., & Maier-Reimer, E. (2002). Advection and removal of 210Pb and stable Pb isotopes in the ocean: A general circulation model study. *Geochim. Cosmochim. Acta*, *66*(2), 257–272.
Hupe, A., & Karstensen, J. (2000). Redfield stoichiometry in Arabian Sea subsurface waters. *Global Biogeochemical Cycles*, *14*(1), 357–372. https://doi.org/10.1029/1999GB900077
Hydes, D. J., & Liss, P. S. (1976). Fluorimetric method for the determination of low concentrations of dissolved aluminium in natural waters. *Analyst*, *101*(922), 922–931. https://doi.org/10.1039/an9760100922
Kalnejais, L. H., Martin, W. R., Signell, R. P., & Bothner, M. H. (2007). Role of sediment resuspension in the remobilization of particulate-phase metals from coastal sediments. *Environmental Science and Technology*, *41*(7), 2282–2288. https://doi.org/10.1021/es061770z
Karstensen, J., & Tomczak, M. (1998). Age determination of mixed water masses using CFC and oxygen data. *Journal of Geophysical Research: Oceans*, *103*(C9), 18599–18609. https://doi.org/10.1029/98JC00889
Kelly, A. E., Reuer, M. K., Goodkin, N. F., & Boyle, E. A. (2009). Lead concentrations and isotopes in corals and water near Bermuda , 1780 – 2000. *Earth and Planetary Science Letters*, *283*(1–4), 93–100. https://doi.org/10.1016/j.epsl.2009.03.045
Klar, J. K., Homoky, W. B., Statham, P. J., Birchill, A. J., Harris, E. L., Woodward, E. M. S., et al. (2017). Stability of dissolved and soluble Fe(II) in shelf sediment pore waters and release to an oxic water column. *Biogeochemistry*. https://doi.org/10.1007/s10533-017-0309-x
Kremling, K., & Streu, P. (2001). The behaviour of dissolved Cd, Co, Zn, and Pb in North Atlantic near-surface waters (30° N/60° W - 60° N/2° W). *Deep Sea Res. I*, *48*, 2541–2567.
Kumar, A., Abouchami, W., Galer, S. J. G., Garrison, V. H., Williams, E., & Andreae, M. O. (2014). A radiogenic isotope tracer study of transatlantic dust transport from Africa to the Caribbean. *Atmospheric Environment*, *82*, 130–143. https://doi.org/10.1016/j.atmosenv.2013.10.021
Lambert, C., Nicolas, E., Veron, A., Buatmenard, P., Klinkhammer, G., Lecorre, P., & Morin, P. (1991). Anthropogenic Lead Cycle in the Northeastern Atlantic. *Oceanologica Acta*, *14*(1), 59–66.
Laumond, F., Copin-Montegut, G., Courau, P., & Nicolas, E. (1984). Cadmium, copper and lead in the western Mediterranean Sea. *Marine Chemistry*, *15*(3), 251–261. https://doi.org/10.1016/0304-4203(84)90021-5
Lee, J. M., Boyle, E. A., Gamo, T., Obata, H., Norisuye, K., & Echegoyen, Y. (2015). Impact of anthropogenic Pb and ocean circulation on the recent distribution of Pb isotopes in the Indian Ocean. *Geochimica et Cosmochimica Acta*, *170*, 126–144. https://doi.org/10.1016/j.gca.2015.08.013
Lee, J. M., Boyle, E. A., Suci Nurhati, I., Pfeiffer, M., Meltzner, A. J., & Suwargadi, B. (2014). Coral-based history of lead and lead isotopes of the surface Indian Ocean since the mid-20th century. *Earth and Planetary Science Letters*, *398*, 37–47. https://doi.org/10.1016/j.epsl.2014.04.030
Marani, D., Macchi, G., & Pagano, M. (1995). Lead precipitation in the presence of sulphate and carbonate: Testing of thermodynamic predictions. *Water Research*, *29*(4), 1085–1092. https://doi.org/10.1016/0043-1354(94)00232-V
Mawji, E., Schlitzer, R., Dodas, E., Abadie, C., Abouchami, W., et al. (2015). The GEOTRACES Intermediate Data Product 2014. *Marine Chemistry*, *177*(Part 1), 1–8. https://doi.org/https://doi.org/10.1016/j.marchem.2015.04.005
McCave, I. N., & Hall, I. R. (2002). Turbidity of waters over the Northwest Iberian continental margin. *Progress in Oceanography*, *52*(2–4), 299–313. https://doi.org/10.1016/S0079-6611(02)00012-5
Measures, C. I., & Edmond, J. M. (1988). Aluminium as a tracer of the deep outflow from the Mediterranean. *Journal of Geophysical Research: Oceans*, *93*(C1), 591–595. https://doi.org/10.1029/JC093iC01p00591
Monteiro, C. E., Cardeira, S., Cravo, A., Bebianno, M. J., Sánchez, R. F., & Relvas, P. (2015). Influence of an upwelling filament on the distribution of labile fraction of dissolved Zn, Cd and Pb off Cape São Vicente, SW Iberia. *Continental Shelf Research*, *94*, 28–41. https://doi.org/10.1016/j.csr.2014.12.004
Moore, W. S. (2000). Determining coastal mixing rates using radium isotopes. *Continental Shelf Research*,

20(15), 1993–2007. https://doi.org/10.1016/S0278-4343(00)00054-6
Moore, W. S. (2008). Fifteen years experience in measuring 224Ra and 223Ra by delayed-coincidence counting. *Marine Chemistry*, *109*(3–4), 188–197. https://doi.org/10.1016/j.marchem.2007.06.015
Moore, W. S., & Arnold, R. (1996). Measurement of 223Ra and 224Ra in coastal waters using a delayed coincidence counter. *Journal of Geophysical Research: Oceans*, *101*(C1), 1321–1329. https://doi.org/10.1029/95JC03139
Morton, P. L., Landing, W. M., Hsu, S.-C., Milne, A., Aguilar-Islas, A. M., Baker, A. R., et al. (2013). Methods for the sampling and analysis of marine aerosols: results from the 2008 GEOTRACES aerosol intercalibration experiment. *Limnology and Oceanography: Methods*, *11*(2), 62–78. https://doi.org/10.4319/lom.2013.11.62
Muller, F. L. L. (1996). Interactions of copper, lead and cadmium with dissolved colloidal and particulate compoenents of estuarine and coastla waters. *Marine Chemistry*.
Muller, F. L. L., Tappin, A. D., Statham, P. J., Burton, J. D., & Hydes, D. J. (1994). Trace metal fronts in waters of the Celtic Sea. *Oceanologica Acta*, *17*, 383–396.
Noble, A. E., Echegoyen-Sanz, Y., Boyle, E. A., Ohnemus, D. C., Lam, P. J., Kayser, R., et al. (2015). Dynamic variability of dissolved Pb and Pb isotope composition from the U.S. North Atlantic GEOTRACES transect. *Deep-Sea Research Part II: Topical Studies in Oceanography*, *116*, 208–225. https://doi.org/10.1016/j.dsr2.2014.11.011
Nozaki, Y., & Tsunogai, S. (1976). 226Ra, 210Pb and 210Po disequilibria in the Western North Pacific. *Earth and Planetary Science Letters*, *32*(2), 313–321. https://doi.org/https://doi.org/10.1016/0012-821X(76)90071-6
Nriagu, J. O., & Pacyna, J. M. (1988). Quantitative assessment of worldwide contamination of air, water and soils by trace metals. *Nature*, *333*, 134.
Obata, H., Karatani, H., & Nakayama, E. (1993). Automated determination of iron in seawater by chelating resin concentration and chemiluminescence detection. *Analytical Chemistry*, *65*(11), 1524–1528. https://doi.org/10.1021/ac00059a007
Ohnemus, D. C., Auro, M. E., Sherrell, R. M., Lagerström, M., Morton, P. L., Twining, B. S., et al. (2014). Laboratory intercomparison of marine particulate digestions including Piranha: a novel chemical method for dissolution of polyethersulfone filters. *Limnology and Oceanography: Methods*, *12*(8), 530–547. https://doi.org/10.4319/lom.2014.12.530
Olsen, A., Key, R. M., van Heuven, S., Lauvset, S. K., Velo, A., Lin, X., et al. (2016). The Global Ocean Data Analysis Project version 2 (GLODAPv2) – an internally consistent data product for the world ocean. *Earth System Science Data*, *8*(2), 297–323. https://doi.org/10.5194/essd-8-297-2016
Pohl, C., Croot, P. L., Hennings, U., Daberkow, T., Budeus, G., & v.d. Loeff, M. R. (2011). Synoptic transects on the distribution of trace elements (Hg, Pb, Cd, Cu, Ni, Zn, Co, Mn, Fe, and Al) in surface waters of the Northern- and Southern East Atlantic. *Journal of Marine Systems*, *84*(1–2), 28–41. https://doi.org/10.1016/j.jmarsys.2010.08.003
Pollard, R. T., Read, J. F., Holliday, N. P., & Leach, H. (2004). Water masses and circulation pathways through the Iceland Basin during Vivaldi 1996. *Journal of Geophysical Research: Oceans*, *109*(C4), n/a-n/a. https://doi.org/10.1029/2003JC002067
Prego, R., Santos-Echeandía, J., Bernárdez, P., Cobelo-García, A., & Varela, M. (2013). Trace metals in the NE Atlantic coastal zone of Finisterre (Iberian Peninsula): Terrestrial and marine sources and rates of sedimentation. *Journal of Marine Systems*, *126*, 69–81. https://doi.org/10.1016/j.jmarsys.2012.05.008
Rapp, I., Schlosser, C., Rusiecka, D., Gledhill, M., & Achterberg, E. P. (2017). Automated preconcentration of Fe, Zn, Cu, Ni, Cd, Pb, Co, and Mn in seawater with analysis using high-resolution sector field inductively-coupled plasma mass spectrometry. *Analytica Chimica Acta*, *976*, 1–13. https://doi.org/10.1016/j.aca.2017.05.008
Rivera-Duarte, I., & Flegal, A. R. (1994). Benthic lead fluxes in San Francisco Bay, California, USA. *Geochimica et Cosmochimica Acta*, *58*(15), 3307–3313. https://doi.org/10.1016/0016-7037(94)90059-0
Rolison, J. M. (2016). *The biogeochemistry of trace metals and their isotopes in the Mediterranean and Black Seas*. (Doctoral dissertation thesis). University of Otago.
Rolison, J. M., Middag, R., Stirling, C. H., Rijkenberg, M. J. A., & de Baar, H. J. W. (2015). Zonal distribution of dissolved aluminium in the Mediterranean Sea. *Marine Chemistry*, *177*, 1–14. https://doi.org/10.1016/j.marchem.2015.05.001
Ryan, W. B. F., Carbotte, S. M., Coplan, J. O., O'Hara, S., Melkonian, A., Arko, R., et al. (2009). Global Multi-Resolution Topography synthesis. *Geochemistry, Geophysics, Geosystems*, *10*(3), n/a-n/a. https://doi.org/10.1029/2008GC002332
Sañudo-Wilhelmy, S. a., & Flegal, A. R. (1994). Temporal variations in lead concentrations and isotopic composition in the Southern California Bight. *Geochimica et Cosmochimica Acta*, *58*(15), 3315–3320. https://doi.org/10.1016/0016-7037(94)90060-4

Schaule, B. K., & Patterson, C. C. (1983). Perturbations of the Natural Lead Depth Profile in the Sargasso Sea by Industrial Lead BT - Trace Metals in Sea Water. In C. S. Wong, E. Boyle, K. W. Bruland, J. D. Burton, & E. D. Goldberg (Eds.) (pp. 487–503). Boston, MA: Springer US. https://doi.org/10.1007/978-1-4757-6864-0_29

Schlitzer, R. (2015). Ocean Data View, http://odv.awi.de. http://odv.awi.de.

Sen, T. K., & Khilar, K. C. (2006). Review on subsurface colloids and colloid-associated contaminant transport in saturated porous media. *Advances in Colloid and Interface Science*, *119*(2–3), 71–96. https://doi.org/10.1016/j.cis.2005.09.001

Sherrell, R. M., Boyle, E. A., & Hamelin, B. (1992). Isotopic Equilibration Between Dissolved and Suspended Particulate Lead in the Atlantic Ocean: Evidence From 210 Pb and Stable Pb Isotopes. *Journal of Geophysical Research*, *97*(C7), 11257–11268. https://doi.org/10.1029/92JC00759

Sun, Y., & Torgersen, T. (1998). The effects of water content and Mn-fiber surface conditions on measurement by emanation. *Marine Chemistry*, *62*, 299–306. https://doi.org/10.1016/S0304-4203(98)00019-X

Talley, L. D., & McCartney, M. S. (1982). Distribution and Circulation of Labrador Sea Water. *Journal of Physical Oceanography*, *12*(11), 1189–1205. https://doi.org/10.1175/1520-0485(1982)012<1189:DACOLS>2.0.CO;2

Véron, A. J., & Church, T. M. (1997). Use of stable lead isotopes and trace metals to characterize air mass sources into the eastern North Atlantic. *Journal of Geophysical Research*, *102*(D23), 28049. https://doi.org/10.1029/97JD01527

Waeles, M., Riso, R. D., Maguer, J. F., Guillaud, J. F., & Le Corre, P. (2008). On the distribution of dissolved lead in the Loire estuary and the North Biscay continental shelf, France. *Journal of Marine Systems*, *72*(1–4), 358–365. https://doi.org/10.1016/j.jmarsys.2007.01.012

Waugh, D. W., Hall, T. M., & Haine, T. W. N. (2003). Relationships among tracer ages. *Journal of Geophysical Research: Oceans*, *108*(C5), n/a-n/a. https://doi.org/10.1029/2002JC001325

Wu, J. F., & Boyle, E. A. (1997). Lead in the western North Atlantic Ocean: Completed response to leaded gasoline phaseout. *Geochimica Et Cosmochimica Acta*, *61*(15), 3279–3283. https://doi.org/10.1016/s0016-7037(97)89711-6

Wu, J., Rember, R., Jin, M., Boyle, E. A., & Flegal, A. R. (2010). Isotopic evidence for the source of lead in the North Pacific abyssal water. *Geochimica et Cosmochimica Acta*, *74*(16), 4629–4638. https://doi.org/10.1016/j.gca.2010.05.017

Zago, C., Capodaglio, G., Ceradini, S., Ciceri, G., Abelmoschi, L., Soggia, F., et al. (2000). Benthic fluxes of cadmium, lead, copper and nitrogen species in the northern Adriatic Sea in front of the River Po outflow, Italy. *Science of the Total Environment*, *246*(2–3), 121–137. https://doi.org/10.1016/S0048-9697(99)00421-0

Zurbrick, C. M., Boyle, E. A., Kayser, R., Reuer, M. K., Wu, J., Planquette, H., et al. (2018). Dissolved Pb and Pb isotopes in the North Atlantic from the GEOVIDE transect (GEOTRACES GA-01) and their decadal evolution. *Biogeosciences Discussions*, 1–34. https://doi.org/10.5194/bg-2018-29

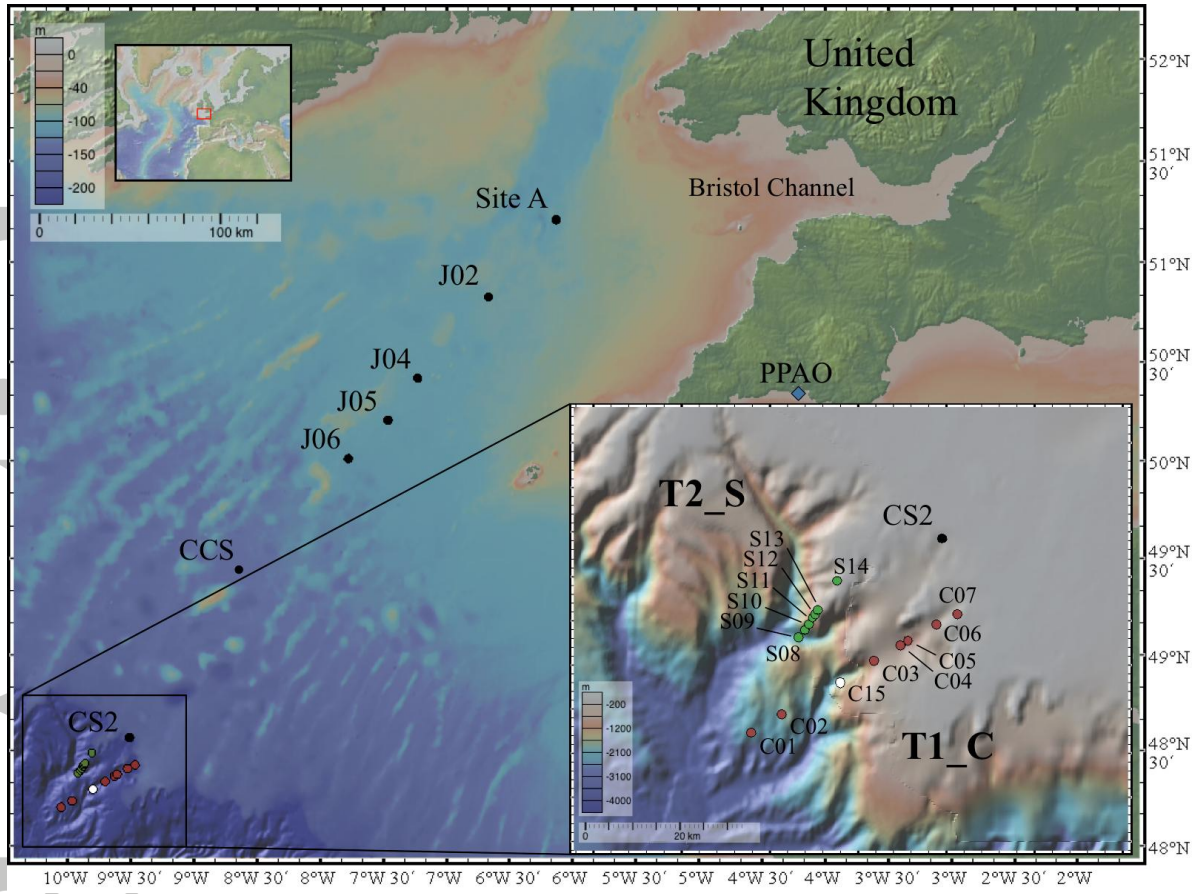

Figure 1. Station locations across canyon T1_C (white and red circles), spur T2_S (green circles) transects and on-shelf transect (black circle) during three research expeditions in November (DY018), April (DY029) and July (DY033). Blue diamond represents PPAO station. Map generated using GeoMapApp, http://www.geomapapp.org (Ryan et al. 2009).

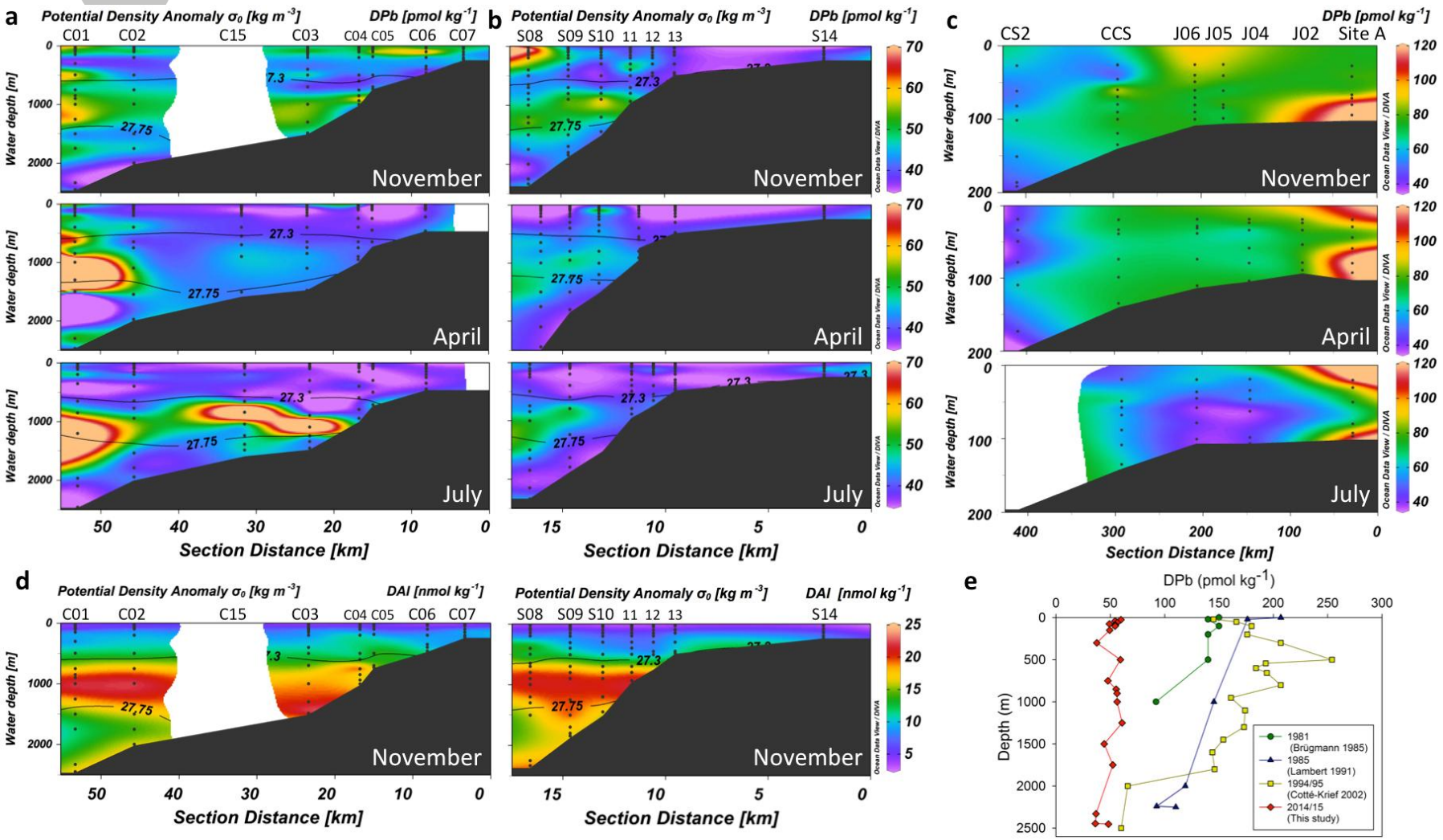

Figure 2. Upper panel: dissolved lead distribution plots (a) along the canyon transects (T1_C, left), (b) along the spur transects (T2_S, middle), (c) and along the on-shelf transect (left) in November (DY018) (top), April (DY029) (middle) and July (DY033) (bottom). Bottom panel: (d) example of dissolved aluminium distribution plots from November (DY018) along the canyon (T1_C) transect (left) and spur (T2_S) transect (right). For the full dissolved aluminium results please see SI, Fig. S2. Black lines

represent MOW density range contour plots. (e) Reduction of DPb concentrations in the Celtic Sea slope region over the last 30 years. Data are from: (Brügmann et al. 1985) green circles, (Lambert et al. 1991) blue triangles, (Cotté-Krief et al. 2002) yellow squares, and this study is represented by the S08 station in April (DY029) by red diamonds.

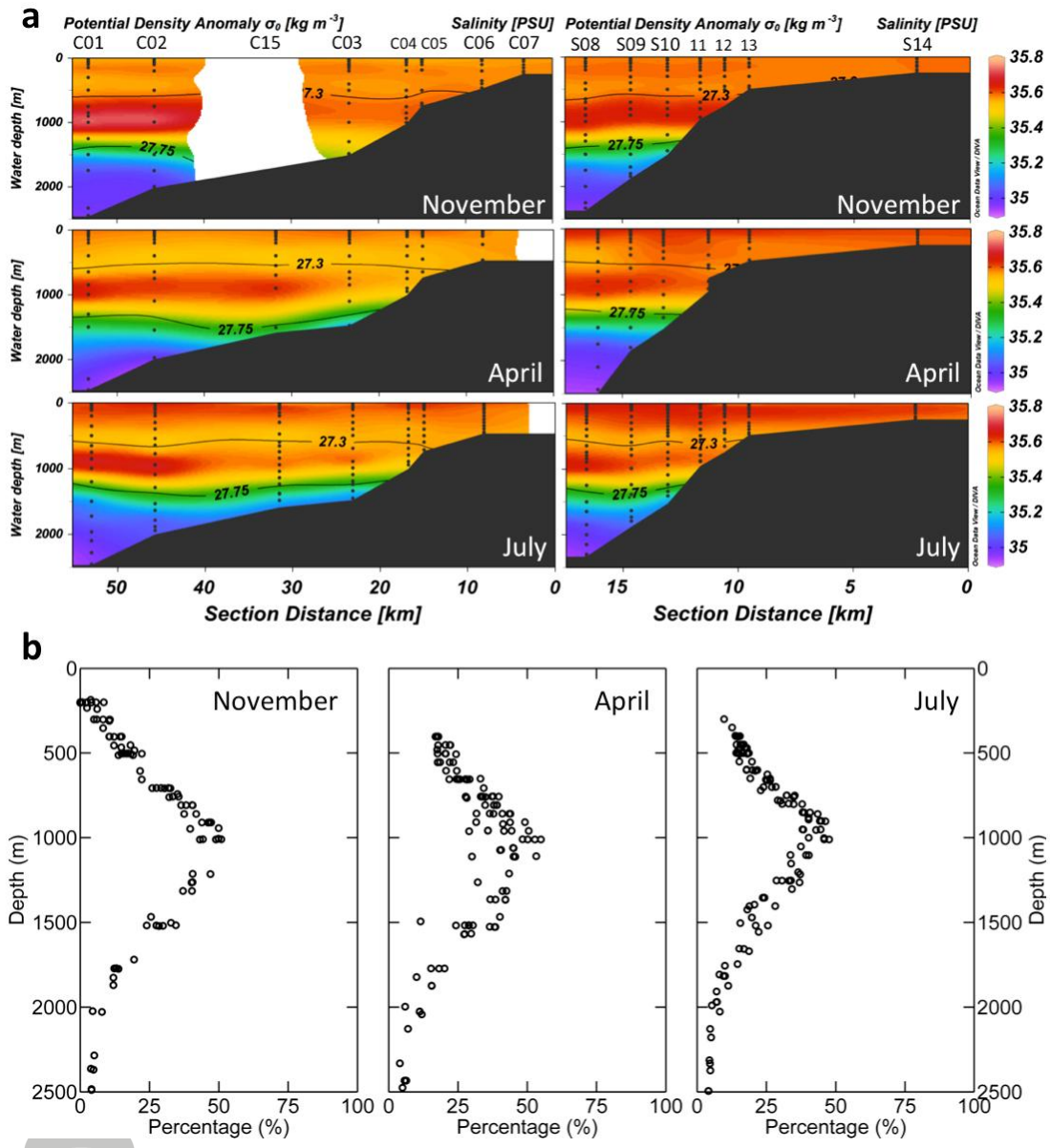

Figure 3. Upper panel (a): salinity distribution plots along the canyon transects (T1_C, left) and along the spur transects (T2_S, right) in November (DY018) (top), April (DY029) (middle) and July (DY033) (bottom). Bottom panel (b): the percentage distribution of MOW along the canyon (T1_C) and spur (T2_S) transects in November (DY018) (left), April (DY029) (middle) and July (DY033) (left). For the full OMP results see SI, Fig. S4.

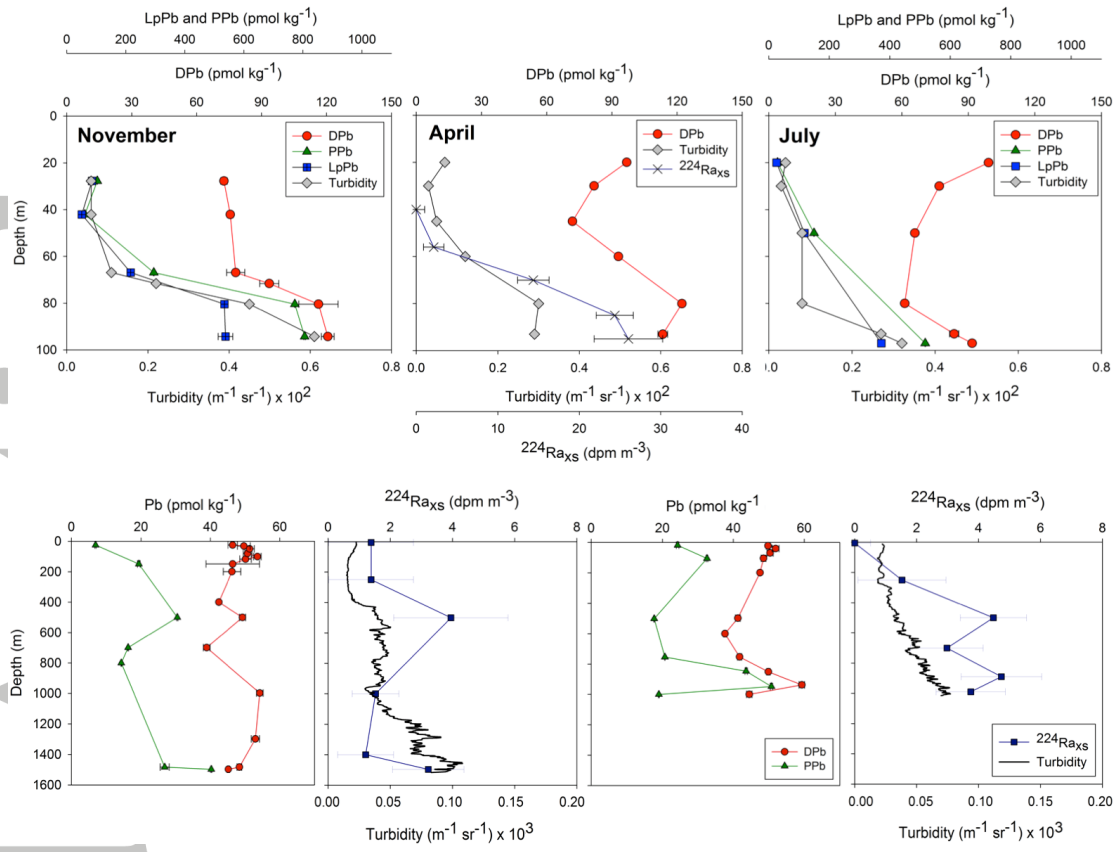

Figure 4. Upper panel: depth profiles of DPb (circles), PPb (triangles), LpPb (squares), turbidity (diamonds) and $^{224}Ra_{xs}$ (crosses) at Site A in November (DY018) (left), April (DY029) (middle) and July (DY033) (left). Bottom panel: depth profiles of DPb (circles), PPb (triangles), $^{224}Ra_{xs}$ (squares) and turbidity (black line) at station C03 (left) and C04 (right) in November (DY018).